

Orientation-controllable self-organized microgratings induced in the bulk SrTiO₃ crystal by a single femtosecond laser beam

Juan Song,^{1,2} Xinshun Wang,^{1,2} Xiao Hu,^{1,2} Jian Xu,^{1,2} Yang Liao,^{1,2} Haiyi Sun,¹ Jianrong Qiu,^{3*} and Zhizhan Xu^{1**}

¹Shanghai Institute of Optics and Fine Mechanics, Chinese Academy of Sciences, Shanghai, 201800, China

²Graduate School of the Chinese Academy of Sciences, Beijing, 100039, China

³Department of Materials Science and Engineering, Zhejiang University, Hangzhou, 310027, China

*Corresponding author: qjr@zju.edu.cn

**Corresponding author: zzxu@mail.shnc.ac.cn

Abstract: Self-organized microgratings were induced in the bulk SrTiO₃ crystal by readily scanning the laser focus in the direction perpendicular to the laser propagation axis. The groove orientations of those gratings could be controlled by changing the irradiation pulse number per unit scanning length, which could be implemented either through adjusting the scanning velocity at a fixed pulse repetition rate or through varying the pulse repetition rate at a fixed scanning velocity. This high-speed method for fabrication of microgratings will have many potential applications in the integration of micro-optical elements. The possible formation mechanism of the self-organized microgratings is also discussed.

©2007 Optical Society of America

OCIS codes: (050.6875) Three-dimensional fabrication; (220.4000) Microstructure fabrication; (320.2250) Femtosecond phenomena

References and links

1. E. V. Pstryakov, A. I. Alimpiev, and V. N. Matrosov, "Prospects for the development of femtosecond laser systems based on beryllium aluminate crystals doped with chromium and titanate ions," *Quantum Elect.* **31**, 689-696 (2001).
2. K. M. Davis, K. Miura, N. Sugimoto and K. Hirao, "Writing waveguides in glass with a femtosecond laser," *Opt. Lett.* **21**, 1729-1731 (1996).
3. H. Sun, Y. Xu, S. Juodkazis, K. Sun, M. Watanabe, S. Matsuo, H. Misawa, and J. Nishii, "Arbitrary-lattice photonic crystals created by multiphoton microfabrication," *Opt. Lett.* **26**, 325-327 (2001).
4. J. Qiu, C. Zhu, T. Nakaya, J. Si, F. Ogura, K. Kojima, and K. Hirao, "Space-selective valence state manipulation of transition metal ions inside glasses by a femtosecond laser," *Appl. Phys. Lett.* **79**, 3567-3569 (2001).
5. B. Tan, Narayanswamy, R. Sivakumar and K. Venkatakrishnan, "Direct grating writing using femtosecond laser interference fringes formed at the focal point," *J. Opt. A* **7**, 169-174 (2005).
6. Q. Z. Zhao, J. R. Qiu, X. W. Jiang, C. J. Zhao, and C. S. Zhu, "Fabrication of internal diffraction gratings in calcium fluoride crystals by a focused femtosecond laser," *Opt. Express* **12**, 742-746 (2004).
7. C. W. Smelser, D. Grobnc, and S. J. Mihailov, "Generation of pure two-beam interference grating structures in an optical fiber with a femtosecond infrared source and a phase mask," *Opt. Lett.* **29**, 1730-1732 (2004).
8. V. R. Bhardwaj, E. Simova, P. P. Rajeev, C. Hnatovsky, R. S. Taylor, D. M. Rayner, and P. B. Corkum, "Optically produced arrays of planar nanostructures inside fused silica," *Phys. Rev. Lett.* **96**, 057404 (2006).
9. Y. Shimotsuma, P. G. Kazansky, J. R. Qiu, and K. Hirao, "Self-organized nanogratings in glass irradiation by ultrashort light pulses," *Phys. Rev. Lett.* **91**, 247405 (2003).
10. W. J. Yang, E. Bricchi, P. G. Kazansky, J. Bovatsek and A. Y. Arai, "Self-assembled periodic subwavelength structures by femtosecond laser direct writing," *Opt. Express* **14**, 10117-10124 (2006).
11. C. Hnatovsky, E. Simova, P. P. Rajeev, D. M. Rayner, P. B. Corkum, and R. S. Taylor, "Femtosecond laser writing of porous capillaries inside fused silica glass," *Opt. Lett.* **32**, 1459-1461 (2007).
12. J. Song, X. S. Wang, J. Xu, H. Y. Sun, Z. Z. Xu, and J. R. Qiu, "Microstructures induced in the bulk of SrTiO₃ crystal by a femtosecond laser," *Opt. Express* **15**, 2341-2347 (2007).

1. Introduction

In recent times, there is a rapid development in ultrafast laser technology [1], the field of femtosecond laser processing is extended to wider applications [2-4]. Among these applications, periodic micro-/nano-structuring of materials attracts special attention for its potential value in all-optical circuits. Traditionally, one way for fabricating a grating is, to employ a two-beam interference configuration [5], and an alternative way is to scan the focal spot of the laser beam line by line [6]. Obviously, the former method is technically complex because of its high requirement for the spatial and temporal alignment between two laser beams, while the latter one is very time-consuming. In this paper, we have reported a kind of self-organized micrograting induced in the bulk SrTiO₃ crystal by a near-infrared femtosecond laser. Here, we have reported a much more simple method for fabricating gratings in the bulk SrTiO₃ crystal: by translating the laser focal point perpendicular to the beam propagation direction, a regular grating was self-fabricated in the side face. Although the interior self-organized gratings have been reported inside fused silica glass both in the light propagation direction and in the plane perpendicular to the laser beam axis [7-11], to the best of our knowledge, it is the first time that a regular large-area self-organized micrograting is observed in the plane determined by the translation direction and the light propagation direction.

2. Experimental setup

The schematic graph of the experimental setup has been presented in our previous work [12]. 120-fs laser pulses, which were delivered from a Ti: sapphire amplifier at a wavelength of 800 nm and at 1 kHz pulse repetition rate, were tightly focused into the bulk SrTiO₃ crystal by a high-numerical-aperture (NA=0.9) microscope objective (100×). The pulse energy could be adjusted by a neutral-density filter and be monitored by an energy meter. The pulse number could be controlled by an electric light shutter. CCD captured the optical micrographs of the sample, and transmitted them to a monitor where the fabrication process was displayed.

In our experiment, the sample was a piece of SrTiO₃ single crystal grown by the flame-fusion method. SrTiO₃ crystal, whose high refractive index of 2.34 helps to heavily increase the refractive index contrast with respect to voids fabricated inside it, has considerable potential to function as photonic crystal. The SrTiO₃ sample with the dimensions of 10mm×10mm×3mm was polished on the (1 0 0) crystal plane for laser irradiation and then polished on the (0 1 0) crystal plane for microscopic observation. The experimental scheme is shown in Fig. 1 in detail: firstly, the laser beam was tightly focused into SrTiO₃ crystal at a fixed depth, and then a straight line was inscribed by translating the laser focus along the y axis in the (1 0 0) crystal plane, perpendicular to the laser beam propagation axis (z-axis). Finally, after laser irradiation, the side facet (y-z plane) was placed under the optical microscope for observation.

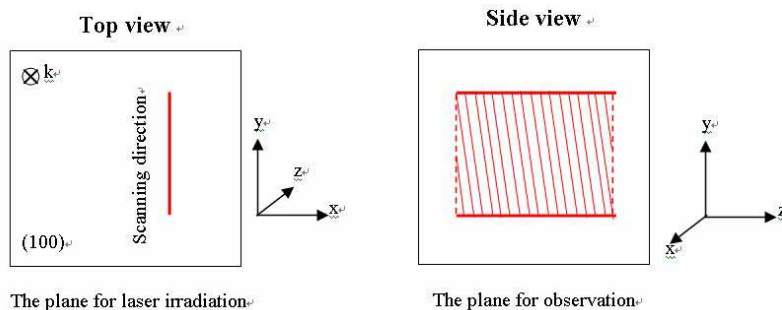


Fig. 1. The schematic graph for femtosecond laser inducing self-organized microgratings in the bulk SrTiO₃ crystal.

3. Experimental results

Figure 2 shows a typical self-organized grating induced in the bulk SrTiO₃ crystal by employing the method mentioned above. The specific experimental parameters were as follows: laser pulses with the energy of 45 μJ were tightly focused through a 100× microscope objective (NA=0.9) into the SrTiO₃ crystal. The laser focus was located at about 200 μm below the sample surface. The scanning velocity was set as 200 μm/s and the laser pulse repetition rate was fixed at 1 kHz. The light beam propagated from left to right. As shown in Fig. 2, except for a few nonparallel grooves at the first beginning, a well regular grating was self-formed with the grooves orientated nearly perpendicular to the laser propagation axis. It is easy for us to extend the size of the grating simply by increasing the scanning distance of the laser beam.

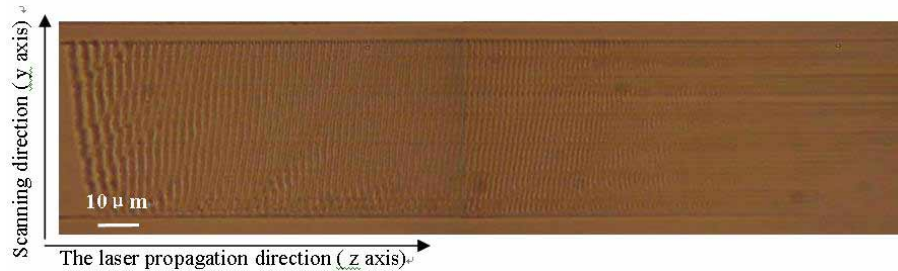


Fig. 2. A typical self-assembled micrograting induced at the focal depth of 200 μm beneath the sample surface by translating the laser focus along the direction perpendicular to the laser beam axis.

We further investigated the influence of the scanning velocities on the formation of the self-assembled microgratings as displayed in Fig. 3. Six different scanning velocities (300 μm/s, 250 μm/s, 200 μm/s, 150 μm/s, 100 μm/s and 50 μm/s) were chosen for comparison. The laser parameters and the focusing conditions were the same as that in Fig. 2. The inset of Fig. 3 shows the schematic of the characterization of the grating structure, where S denotes the scanning direction, g represents the groove orientation, and θ accounts for the angle between them. We define that θ is positive when the grating vector g situates on the left of the scanning direction vector S and negative otherwise. It is clear that with decreasing the scanning velocity, θ turns gradually from negative value to positive value. Interestingly, there exists a critical scanning velocity so that θ nearly approaches zero.

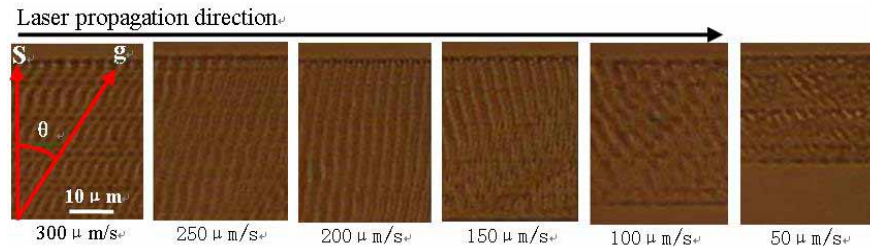


Fig. 3. The dependence of the grating structure on the scanning velocity at a fixed laser pulse repetition rate.

To further verify that the change of the groove orientation with the scanning velocity is an essential physical phenomenon but not a pseudomorph caused by the movement error, we carried out another group of experiments where the stage scanning velocity was fixed at a

constant value of $80\mu\text{m/s}$ while the laser repetition rates were chosen as 166 Hz, 333 Hz, and 500 Hz respectively. The pulse energy used was also $45\mu\text{J}$, and the focal depth was still $200\mu\text{m}$ beneath the sample surface. As shown in Fig. 4, although the scanning velocity was kept unchanged in each case, the induced self-assembled microgratings have very distinct orientation angles θ .

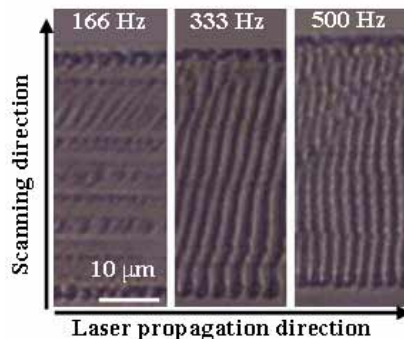


Fig. 4. The influence of the laser pulse repetition rate on the grating structures at a fixed scanning velocity.

Based on two groups of experimental results described above, we conclude that the groove orientation can be varied by changing the irradiation pulse number per unit scanning length.

4. Discussion

Some kinds of self-organized periodic structures inside transparent dielectrics have been reported previously [9-11]. They employed the same transverse direct-writing method as we did. Both groups pointed out that even if the laser focus was fixed inside the samples without translation, there still appeared periodic nanostructures in the cross sections both along and perpendicular to the laser beam propagation direction. Instead, in our case, if the laser focus was fixed, just a self-aligned void array appeared along the laser propagation axis [12] and additional translation of laser focus is needed to induce self-organized periodic microstructures of our kind. In addition, the groove orientations in their cases were controlled by changing the polarization state of the laser beam while in our case by adjusting the pulse number per unit scanning length. Obviously, different formation mechanisms dominated the formation of the self-organized periodic structures.

A typical void string reported in our previous work was presented in Fig. 5 [12]. The experimental method employed here is just the extension of the previous one by simply translating the laser focus along the direction perpendicular to the laser beam axis, so it is reasonable to predict the appearance of a self-assembled grating formed by connection between voids in the adjacent two void strings. It could be suggested that the groove orientation must be just perpendicular to the laser beam propagation direction, but the grating structures displayed in Fig. 3 and Fig. 4 obviously go beyond our imagination. Watanabe et al. demonstrated that even without moving the laser focus, the successive irradiation of femtosecond laser pulses moved a microscopic bubble against the laser propagation direction inside crystalline calcium fluoride and amorphous silica glass [13]. We have developed a phenomenal model based on their experimental results. As illustrated in Fig. 6, adjacent void strings are differentiated by red color and green color respectively, and the voids in each void string are labeled with different Arabic numbers in sequence. The light beam propagates from left to right and the scanning direction is indicated with red arrow in Fig. 6. In our case, the void diameter was generally larger than $1\mu\text{m}$ and the scanning velocity employed here ensured that at least two pulses irradiated the damage spot with the size of $1\mu\text{m}$, so the adjacent void strings are believed to be overlapped with each other. Hence, for the formation

of the second void string, when the first pulse comes [the case in Fig. 6(a)], the breakdowns where new voids will be generated are most likely to occur at the upper left corners of the voids in the first string because of the lower damage threshold caused by color center or defects at the interface between the voids and the SrTiO₃ substrate. Different scanning velocities correspond to different laser shots per unit scanning length, and the higher the velocity, the less the laser shots. At a relatively high scanning velocity, although just a few pulses contribute to the formation of the void strings, the No. 2 void in the second string can be moved toward the left by the laser pulses to depart from the No. 2 void in the first string, catch and finally adhere to the upper right corner of the No. 1 void in the first string, as is the case in Fig. 6(b). When we adopt a moderate scanning velocity where more pulses continue to have effects on the existing void in Fig. 6(b), the No. 2 void in the second string will be moved toward the laser focus further so that at a certain velocity, the No. 2 void in the second string and the No.1 void in the first string will be aligned in a line perpendicular to the laser beam axis by coincidence, just as Fig. 6(c) shows. When the scanning velocity is lower [the case in Fig. 6 (d)], the additional pulses will make the red No.2 void in Fig. 6(c) continue to move towards the left so that the No. 2 void in the second string finally surpasses the No.1 void in the first string and becomes attached to its upper left corner. The purple dashed lines in Fig. 6 indicate the groove orientation in each case, which coincides well with the experimental phenomenon. In addition, since Prof. Watanabe demonstrated that larger pulse energy led to faster motion rate of bubbles (defined as moving distance per pulse), it is easy for us to understand the orientation differences shown in Fig. 3 between the start of the grating and the uniform part of it. Therefore, not only the irradiation pulse number per unit scanning length but also pulse energy can have influence on the groove orientations of the gratings.



Fig. 5. A typical void string induced in the bulk SrTiO₃ crystal by tightly focusing fs laser pulses through a 100× microscope objective.

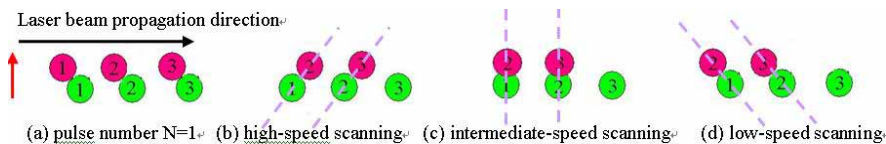


Fig. 6. The schematic of a void-moving model.

To support the above conjecture, the following experiment was carried out. The femtosecond laser pulses with the energy of 30 μJ were tightly focused into the SrTiO₃ crystal at a focal depth of 200 μm beneath the sample surface, and the scanning velocity was set as 250 μm/s. Two lines were written along the axis perpendicular to the laser beam axis, but difference between them is that one was written along the y+ direction and the other was written along the y- direction. The induced grating structures are presented in Fig. 7, where red arrows indicate the scanning directions. It is clear that the groove orientations in two cases are both tilted and well symmetric with respect to the laser propagation direction (z axis). This symmetry could be easily understood by employing our void-moving model, just as Fig. 8 demonstrates.

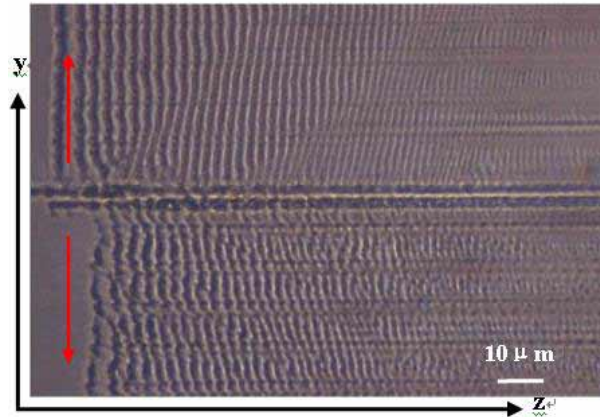


Fig. 7. Two different grating structures induced by scanning the laser focus in two opposite directions.

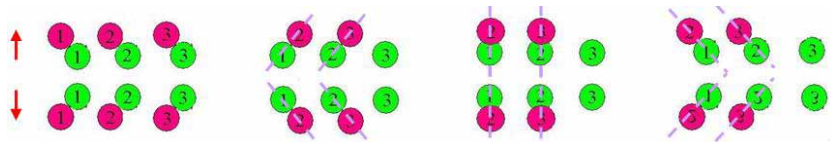


Fig. 8. The schematic of how the symmetry is formed.

Our previous study indicated that the void string length could be changed distinctly through adjusting the focal depth, and the size uniformity of the voids can be optimized by choosing an appropriate focal depth [12]. Therefore, it is possible to improve the quality of the orientation-controllable self-assembled microgratings by careful adjustment of the combination of the laser parameters and the focusing conditions.

5. Conclusion

In this paper, we have reported a kind of self-assembled micrograting induced in the bulk SrTiO₃ crystal by translating a tightly-focused laser beam along the axis perpendicular to the laser propagation direction. The groove orientation of the micrograting could be controlled by changing the laser pulse number per unit scanning length. A void-moving model is proposed to qualitatively explain the formation mechanism of the grating as well as the variation of the groove orientation. This method for fabrication of gratings has the advantages of being mask free, high efficiency, selectivity and localizability, and it has high potential for applications in fabricating large-area gratings inside transparent dielectrics.

Acknowledgment

This work was supported by the National Basic Research Program of China (No. 2006CB806000).